



## Synthesis of Waste Paper Based Novel Aerogel for the Removal of Dyes from Textile Industry Effluent

*I. Anjali<sup>1</sup>, N. Prasanna Gayatri<sup>2</sup>, T. Jaya Raj<sup>3</sup>, D. Kumar<sup>4</sup>, K. Ratna Kumar<sup>5</sup>, Dr. Tapas Kumar<sup>6</sup>*

<sup>1,2,3,4,5</sup> UG Student, <sup>6</sup>Guide, Associate professor

Department of Chemical Engineering, GMR Institute of Technology, Rajam, Andhra Pradesh, India

### ABSTRACT

Various adsorbents have been developed to deal with industrial dyes, however those are not widely used as they were uneconomical and non-regenerable. renewable resources are usually preferred for aerogel synthesis due to their biocompatible properties and eco-friendly nature. A renewable tissue paper-based cellulosic aerogel was synthesized in a modest, economical, and simply scalable freeze-drying method. Cellulose-based aerogels have unique properties like low density, high porosity, light in weight, and enormously stiff, and can easily bear the weight. Furthermore, the aerogel also exhibited a low thermal conductivity (0.017– 0.038 W/mK). Thus, the synthesized aerogel was found to be an eco-friendly. Thus, the novelty of the present work lies in the fact that waste tissue paper-derived aerogel is biodegradable, non-toxic, thermal insulator, and effectively a good dye adsorbent.

**Keywords:** Aerogel, WTPA (Waste Tissue Paper Aerosol), MB dye(Methylene Blue), Porosity, Adsorption.

## 1. INTRODUCTION

### 1.0. Introduction

Industries create substantial effluent and being discharged to the different water bodies and thereby creating severe menace for aquatic life and mankind.

One of the main sources with severe pollution problems worldwide is textile industry effluent containing synthetic dyes and other auxiliary chemicals.

Table.1. Effluent Generation for Different Specific Sectors

(Source: <https://indianinfrastructure.com/2020/02/01/wastewater-generation-and-treatment- present-status-in-india/>)

Sector Specific	Total Units	Effluent Generation (MLD)
Chemical	27	97.8
Distillery	35	37.0
Food, Diary & Beverage	22	6.5
Pulp & Paper	67	201.4
Sugar	67	96.0
Textile, Bleaching&Dye	63	11.4
Tannery	442	22.1
Others	41	28.6

Table.1. shows the effluent generation for different specific sectors in MLD. In which pulp and paper industries has major contribution. Effluent may carry pollutants such as fats, chemicals, detergents, dyes being discharged to the different water bodies and thereby creating severe menace for aquatic life and mankind.

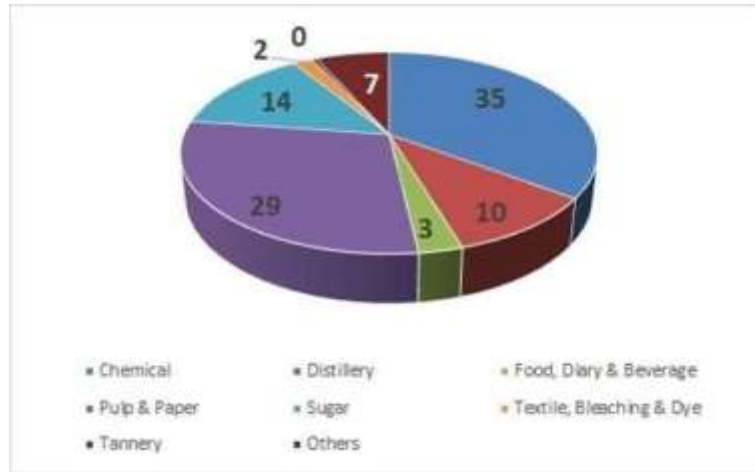


Fig. 1. Industry wise contribution for waste water effluent (Source: Chemical Economics Handbook, 2014)

Fig.1. illustrates the industry wise contribution for wastewater effluent. In which pulp and paper industry has the major contribution followed by chemical, sugar, distillery, tannery, textile, bleaching and dye, food, dairy and beverage industries.

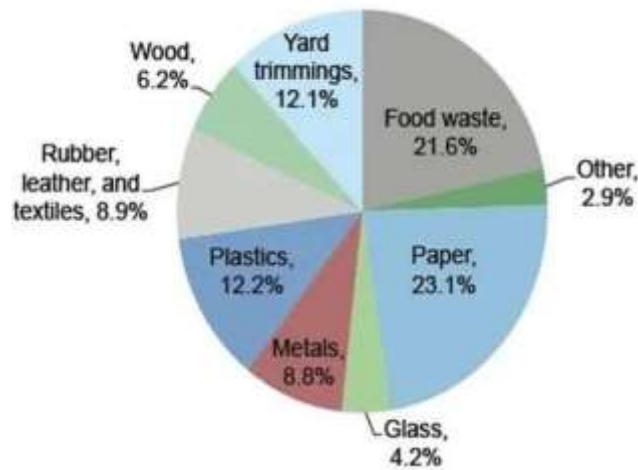


Fig. 2. MSW COMPOSITION

(Source: Chemical Economics Handbook,2014)

Fig.2. illustrates the municipal solid waste the major components of MSW are food waste, paper, plastic, rags, metal, and glass although demolition and construction debris is often included in collected waste, as are small quantities of hazardous waste, such as electric depending on the techniques and technologies applied. And the major water consumption in dyeing industries is for wet processing.

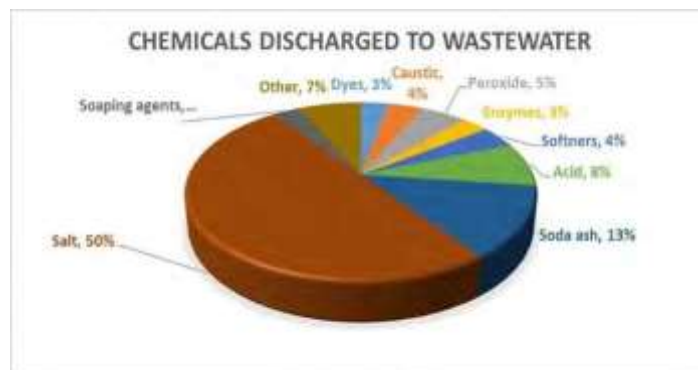


Fig.5. Percentage breakdown of chemical contaminants in textile

(Source: Chemical Economics Handbook, 2014)

Fig.5.illustrates Chemical contaminants is the phrase used to indicate situations where chemicals are either present where they shouldn't be or are at higher concentrations than they naturally have occurred. And the textile industries have chemical contaminants of salts-50%, soda ash-13%, acids-8%, peroxyde-5%, caustic-4%, enzymes-3%, dyes-3%.

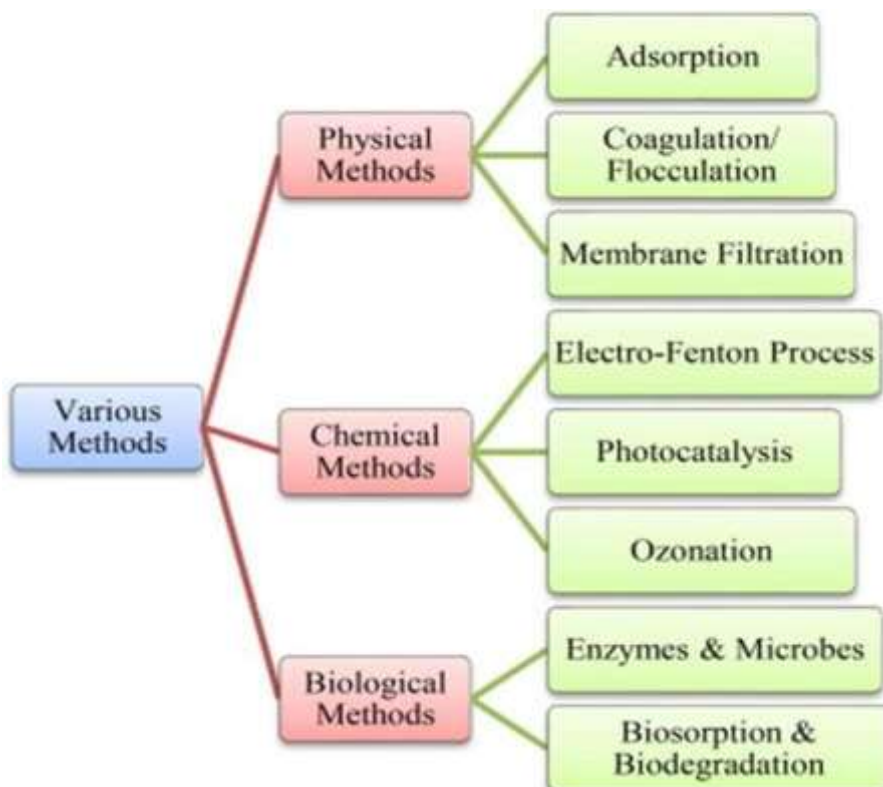


Fig.6 Treatment Methodologies for Textile Industry Effluent

### 3. MATERIALS AND METHODS

#### 3.1 Materials

Waste tissue paper (WTP) was collected from the canteen area at GMRIT campus, Rajam. Polyvinyl alcohol (PVA, 99%), molecular weight 100,000 to 125,000 g/mol having 86–89% degree of hydrolysis, and glyoxal (GLX, ~ 40% content in water) were taken from the laboratory. Other chemicals like hydrochloric acid (HCl, 37%), sodium hydroxide (NaOH, 98%), and ethanol (99%) were collected from the chemistry lab. All solutions were prepared in double-distilled water.

#### 3.2 Treatment of waste tissue paper

The waste tissue paper of 5g was dipped in 500 ml of 0.5wt% HCl solution for 20 h and stirred for 3h. The residual chloride ions were removed from homogenized solution by diluting it with plenty of water. Using suction flask, the pulp was filtered and dried at 70°C in the hot air oven. The pre-treated tissue paper (TP) was obtained which is used in the next step.

#### 3.3 Synthesis of tissue paper aerogel

Pre heated tissue paper (TP) of 0.5g was taken from above step. Stirred it with double distilled water of 50ml for 20-30 min. 6g of PVA solution was prepared in double distilled water(100ml) at 50-60 °C by using magnetic stirrer at 600 rpm for 1h. then we get the clear solution. Now the pre-treated TP pulp and cross linker GLX of 3ml were added to the PVA solution and the stirring was continued at 80°C for 1h. By adding two to three drops of HCl, pH was adjusted to 3. By heating the slurry in the hot oven better cross linking was obtained at 80°C for 3h. Slurry thickness was controlled by the plastic mould and for removal of the air bubbles. The obtained slurry was cooled at -20°C in a deep freezer for 10-12h followed by lyophilization method in a freeze dryer at -55°C for 48h. Hence, the tissue paper aerogel was obtained. The same procedure was followed for all the samples of 1g,1.5g,2g. The schematic diagram for the synthesis of TPA is shown in fig.7b.

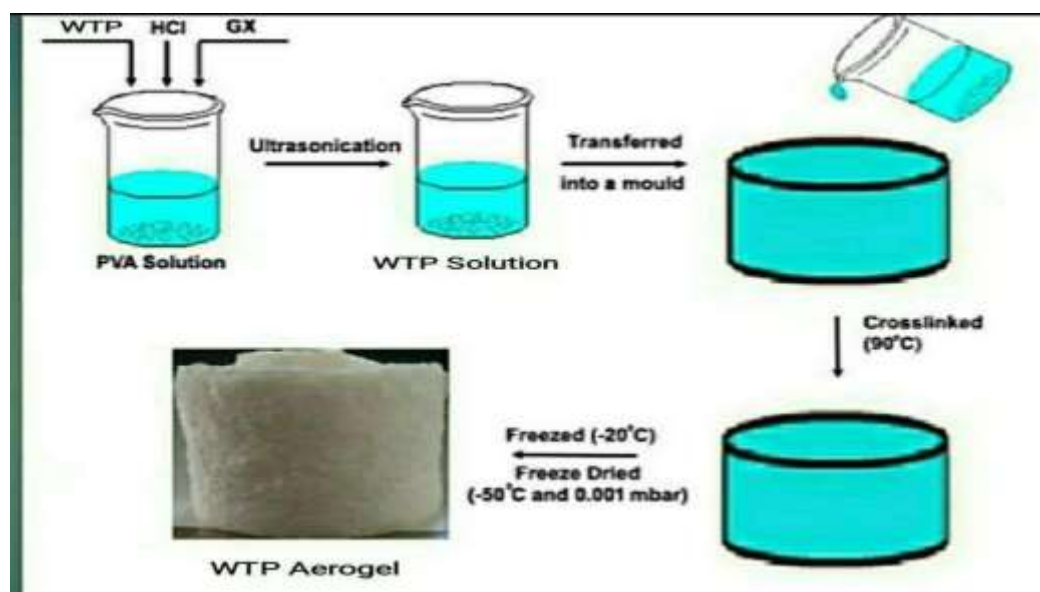


Fig.7. Schematic Diagram of WTPA

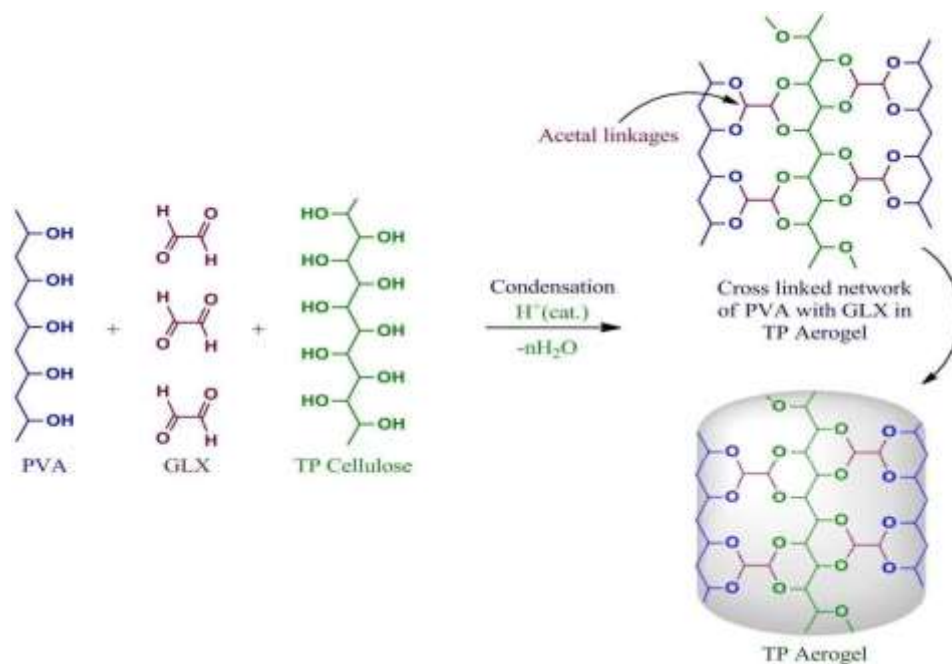


Fig.8. Plausible synthesis mechanism

## 4. RESULTS & DISCUSSION

### 4.0 Results and discussion

#### 4.1 Evaluation of tissue paper aerogel

Ultra-light aerogels were prepared from the renewable waste tissue papers by the cross linking PVA and GLX. The TPAs were prepared by the sol-gel process and moulded into a 3cm × 3 cm cylindrical shape.

#### 4.2 Characterization of waste tissue paper aerogel

The synthesized TPA was placed on the petals of a flower. and it was observed that TPA could stand on the flower without twisting its petals, thereby revealing its ultra-light characteristics. Furthermore, a weight of 2 kg was placed on TPA that could easily withstand the load.



Fig.9. This Images showing of ultra light characteristics of WTPA

The magnified images of the SEM morphologies of the TPA (2 wt%), refer fig.9. The cage-like structure in the TPA morphology indicates the porous architecture of TP fibers, thus confirming their ultra-light characteristics. These magnified images, as shown in Fig.10, also confirm the cross-linking of TP, PVA, and GLX. The irregular pores observed in the SEM morphologies can be attributed to the sample cutting before mounting on the SEM plate.

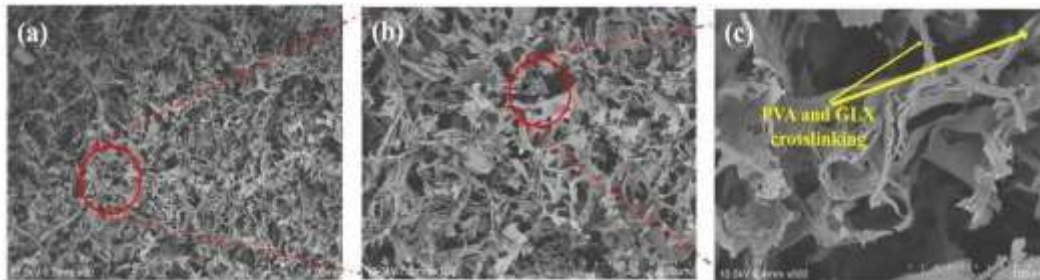


Fig.10. The magnified images of SEM morphology of WTPA

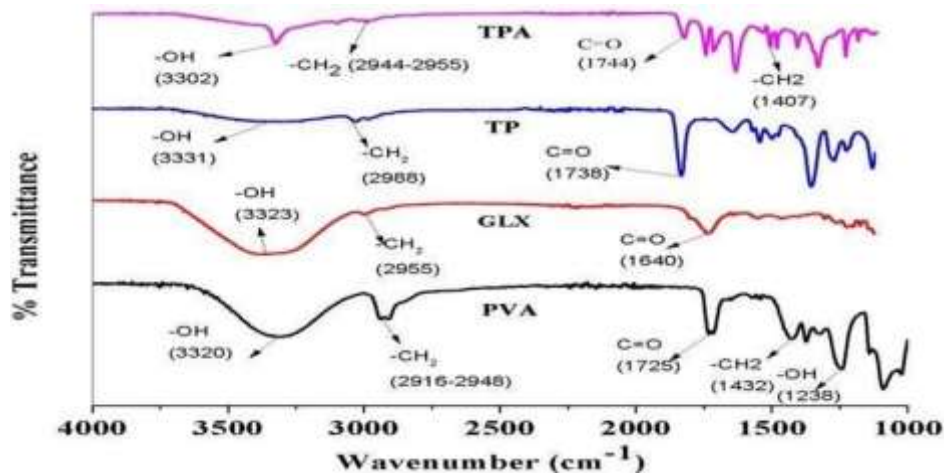


Fig.11 FT-IR spectra of PVA, GLX, TP, and WTPA

After confirming the morphologies from SEM analysis, the synthesis of aerogels was further confirmed to FT-IR spectra (Fig.11). The bands at 3320 cm<sup>-1</sup> correspond to the -OH group and the appearance of the C = O band at 1725 cm<sup>-1</sup> indicates the residual acetaldehyde peak of PVA. The low intense bands at 2916–2948 cm<sup>-1</sup> were attributed to the symmetric and asymmetric stretching of -CH<sub>2</sub>. Similarly, the bending of -CH<sub>2</sub> shows a less intensity

band at  $1432\text{ cm}^{-1}$ . Furthermore, the intense bands observed at  $1725$  and  $1238\text{ cm}^{-1}$  correspond to the stretching frequencies of  $\text{C}=\text{O}$  and  $\gamma\text{-OH}$  due to  $\text{CH}$  wagging, respectively. The band observed at  $1640\text{ cm}^{-1}$  shows the presence of the  $\text{C}=\text{O}$  functional group from GLX. Also, the bands at  $3331\text{ cm}^{-1}$  ( $-\text{OH}$ ),  $2988\text{ cm}^{-1}$  ( $-\text{CH}_2$ ), and  $1738\text{ cm}^{-1}$  ( $\text{C}=\text{O}$ ) were observed for TP. On the other hand, in the FT-IR spectrum of TPA, an intense band was observed at  $3302\text{ cm}^{-1}$  owing to the presence of the free hydroxyl group to maintain better hydrophilicity. The shift in the band values ranging from  $2944$  to  $2955\text{ cm}^{-1}$  for the  $-\text{CH}_2$  stretch confirms the cross-linking of TP with the PVA and GLX. Furthermore, the acetal linkage forms during the crosslinking of TP fiber and PVA chain cause a shift in the  $\text{C}=\text{O}$  group to  $1744\text{ cm}^{-1}$ .

#### 4.3. Cumulative pore size distribution of TPA's

The cumulative pore volumes and pore size for the TPAs were found to be  $2.76$ ,  $2.68$ ,  $2.58$ , and  $2.48\text{ cm}^3/\text{g}$  and  $11.3$ ,  $10.9$ ,  $8.46$ , and  $7.6\text{ nm}$ , as shown in Fig.12. The collapse of macropore and micropores instigate the decrease in pore volume and pore size with an increase in the TP concentrations. The relation with pore volume and pore size are discussed in the table.3.

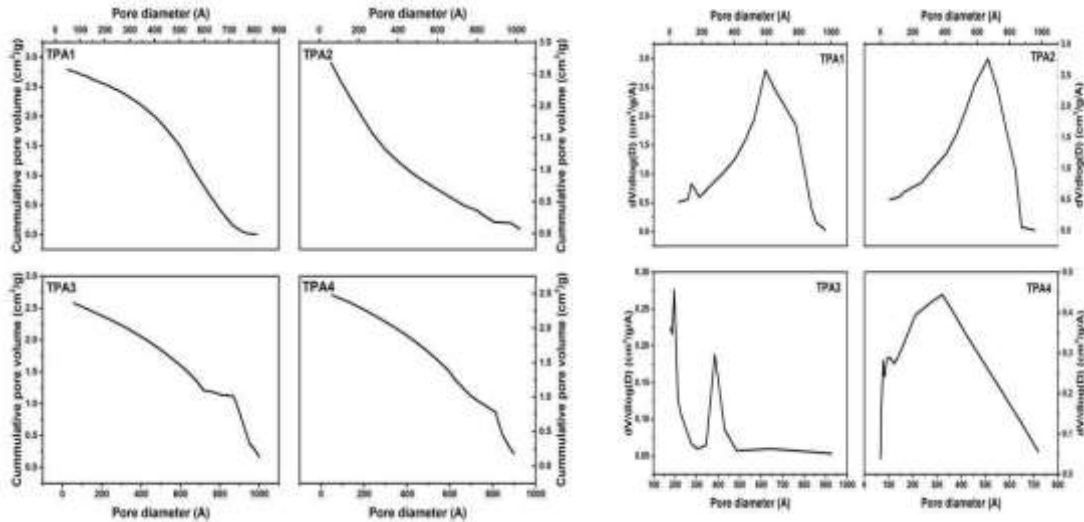


Fig.12. Pore size distribution

#### 4.4 Study on Thermal insulation properties and thermal stability of waste tissue paper aerogel

The thermal conductivities of the synthesized TPAs were measured at room temperature, and the results are in Fig.13.a. The thermal conductivity of the materials depends on the density, moisture, and temperature. The decreased pore volume with an increase in TP concentration reduces the jammed air, which increases the thermal conductivity of TPA. As compared to silica aerogel and sugarcane bagasse aerogel, TPAs possess less thermal conductivity ( $0.017\text{--}0.038\text{ W/mK}$ ).

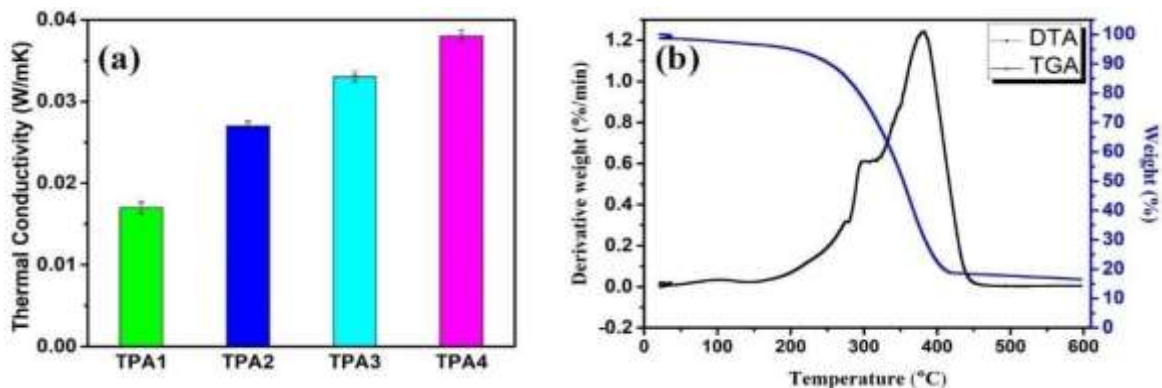


Fig. 13.a. Thermal conductivity of TPAs, 13.b. TGA and DTA analysis of TPA

The thermal stability of the TPA was studied from TGA and DTA analysis (Fig.13.b). The two distinct phases of decomposition of TPA were observed. The first phase comprises a 20% weight degradation between  $250$  and  $275\text{ °C}$  due to the breakdown of the PVA and GLX, whereas the second phase shows 40% degradation between  $325$  and  $350\text{ °C}$ . Above  $375\text{ °C}$ , a marginal weight loss was observed due to TPA conversion into carbonaceous compounds. Thus, the synthesized WTPA can withstand a maximum temperature of  $375\text{ °C}$ , and its low thermal conductivity increases its potential as a high-temperature insulating material.

#### 4.5 Effect of pH on the adsorption capacity of WTP aerogels:

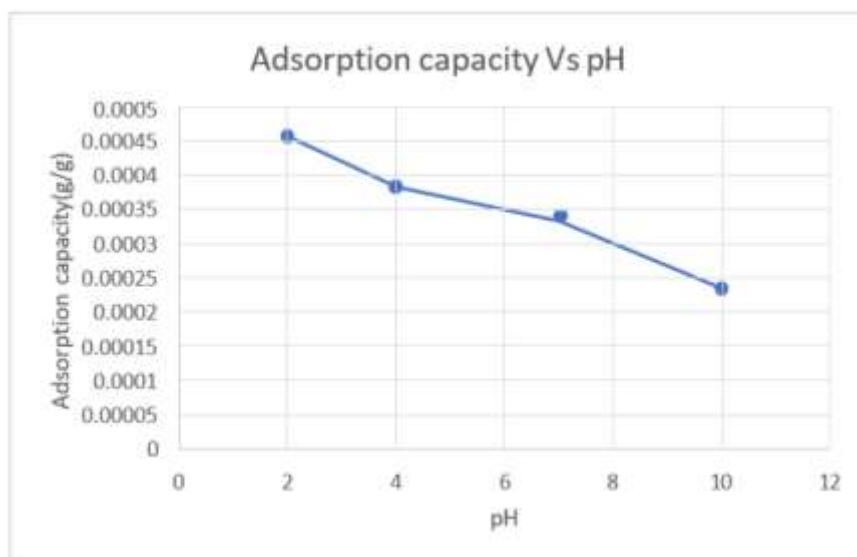


Fig.14 Adsorption Capacity vs pH

The effect of pH of waste tissue paper aerogel on adsorption capacity increases due to the presence of hydrogen ions in the solution, effecting the hydrogen bonding between methylene blue and cellulose fibres. Hence increasing adsorption capacity

#### 4.6 Effect of concentration on the adsorption capacity of WTP aerogels:

The effect of concentration of the dye on the adsorption capacity is shown by Fig.15.

The effect of concentration of waste tissue paper aerogel on adsorption capacity depends on several factors such as the surface area, pore structure, and functional groups present in the aerogel. Generally, increasing the concentration of waste tissue paper aerogel in the adsorption process can lead to higher adsorption capacity due to a larger available surface area for the dye molecules to interact with.

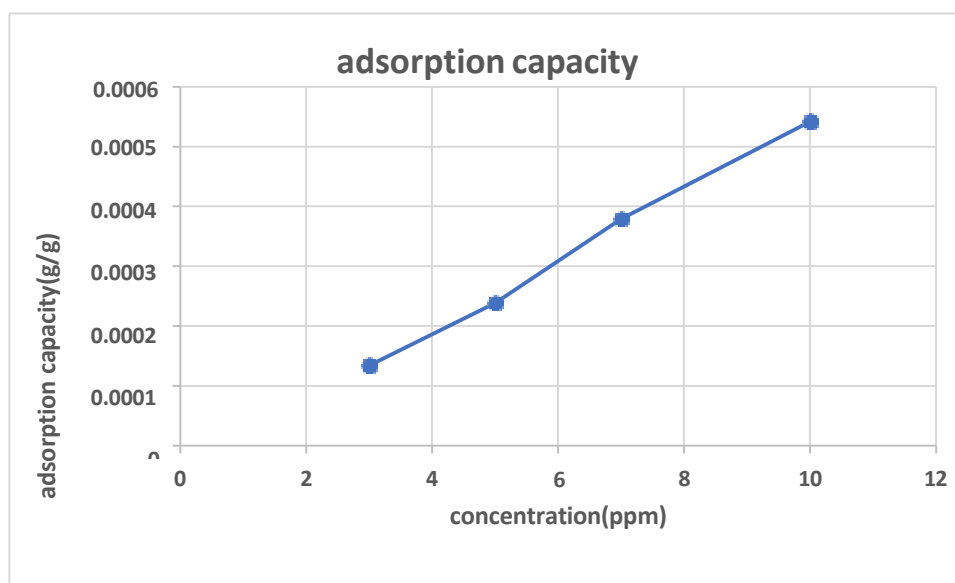


Fig.15 Adsorption capacity vs concentration

#### 4.7 Effect of temperature on the adsorption capacity of WTP aerogels:

Here we can observe the variation in adsorption capacity with changing in temperature. Here in this experimental section, we observed that as the temperatures increases final absorbances and final concentration was increase. But here the adsorption capacity was decreased, it was shown in fig.16. so, we have to take adsorption isotherms into consideration. Further the study on adsorption isotherms must be conducted.

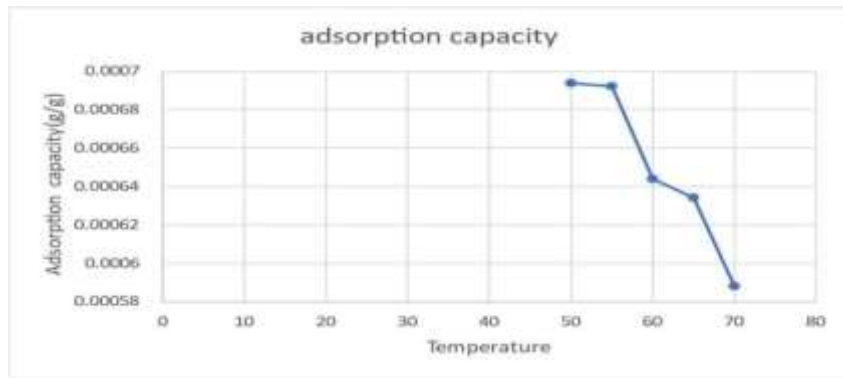


Fig.16. Adsorption Capacity vs Temperature

## 5. CONCLUSION

### 5.0. Conclusion

An ultra-light aerogel was prepared by cross-linking with PVA and GLX using lyophilization method. The aerogel with 2 wt% of tissue paper have shown a better flexibility and light characteristics. It has been observed that by increasing concentration of WTPA, decreasing in porosity, surface area, cumulative pore and volume and also diameter. Moreover, WTPA possesses the lowest thermal conductivity of 0.017 W/mK and thus can be utilized as a thermal insulator. Furthermore, the WTPA of adsorption capacity increases as pH decreases and increase in concentration. And also, it is observed that as temperature increases adsorption capacity of WTP aerogel decreases. Thus, the synthesized aerogel was converted into a high valued product using tissue papers.

### 5.1. Future scope of work

Further work is on Investigation of adsorption kinetics and Comparison of the dye adsorption capacity with the earlier study.

### References

1. K. Chen, Q. Feng, D. Ma, X. Huang, Hydroxyl modification of silica aerogel: An effective adsorbent for cationic and anionic dyes, *Colloids Surfaces A Physicochem. Eng. Asp.* 616 (2021) 126331. <https://doi.org/10.1016/j.colsurfa.2021.126331>.
2. G.P.S. Ibrahim, A.M. Isloor, Inamuddin, A.M. Asiri, N. Ismail, A.F. Ismail, G.M. Ashraf, Novel, one-step synthesis of zwitterionic polymer nanoparticles via distillation-precipitation polymerization and its application for dye removal membrane, *Sci. Rep.* 7 (2017) 1–16. <https://doi.org/10.1038/s41598-017-16131-9>.
3. C. Huang, B. Cai, L. Zhang, C. Zhang, H. Pan, Preparation of iron-based metal-organic framework @cellulose aerogel by in situ growth method and its application to dye adsorption, *J. Solid State Chem.* 297 (2021) 122030. <https://doi.org/10.1016/j.jssc.2021.122030>.
4. M. Rini, M. Rajeev, M. Ashik, Efficiencies of Orange and Lemon Peel in the Removal of Dye From Textile Industry Effluent, (2020) 67–70.
5. T. Wang, J. Cai, J. Zheng, K. Fang, I. Hussain, D.Z. Husein, Facile synthesis of activated biochar/BiVO<sub>4</sub> heterojunction photocatalyst to enhance visible light efficient degradation for dye and antibiotics: applications and mechanisms, *J. Mater. Res. Technol.* 19 (2022) 5017–5036. <https://doi.org/10.1016/j.jmrt.2022.06.177>.
6. Material, O.H. Fadhil, Decolorizing of Malachite Green Dye by Adsorption Using Corn Leaves as (2021) 1–12.
7. M. Ahmad, M. Abdullah, H. Moon, D. Han, Plant Disease Detection in Imbalanced Datasets Using Efficient Convolutional Neural Networks with Stepwise Transfer Learning, *IEEE Access.* 9 (2021) 140565–140580. <https://doi.org/10.1109/ACCESS.2021.3119655>.
8. S. Sharma, A. Kaur, Various methods for removal of dyes from industrial effluents - a review, *Indian J. Sci. Technol.* 1 (2018) 1–21. <https://doi.org/10.17485/ijst/2018/v1i1i2/120847>.
9. B.M. Thamer, A. Aldabhi, M.A. Meera, M.H. El-Newehy, In situ preparation of novel porous nanocomposite hydrogel as effective adsorbent for the removal of cationic dyes from polluted water, *Polymers (Basel).* 12 (2020) 1–18. <https://doi.org/10.3390/polym12123002>.



10. G.B.S. Ibrahim, A.M. Isloor, Inamuddin, A.M. Asiri, N. Ismail, A.F. Ismail, G.M. Ashraf, Novel, one-step synthesis of zwitterionic polymer nanoparticles via distillation-precipitation polymerization and its application for dye removal membrane, *Sci. Rep.* 7 (2017) 1–16. <https://doi.org/10.1038/s41598-017-16131-9>.
11. N.H.N. Do, B.Y. Truong, P.T.X. Nguyen, K.A. Le, H.M. Duong, P.K. Le, Composite aerogels of TEMPO-oxidized pineapple leaf pulp and chitosan for dyes removal, *Sep. Purif. Technol.* 283 (2022) 120200. <https://doi.org/10.1016/j.seppur.2021.120200>.
12. L.X. Cheng, L. Zhang, X.Y. Chen, Z.J. Zhang, Efficient conversion of waste polyvinyl chloride into nano porous carbon incorporated with MnOx exhibiting superior electrochemical performance for supercapacitor application, *Electrochim. Acta.* 176 (2015) 197–206. <https://doi.org/10.1016/J.ELECTACTA.2015.07.007>.
13. Q.B. Thai, D.K. Le, T.P. Luu, N. Hoang, D. Nguyen, H.M. Duong, Aerogels from Wastes and their Applications, *JOJ Mater. Sci.* 5 (2019) 3–6. <https://doi.org/10.19080/JOJMS.2019.05.555663>.
14. Y.H. Peng, A.A. Kashale, Y. Lai, F.C. Hsu, I.W.P. Chen, Exfoliation of 2D materials by saponin in water: Aerogel adsorption / photodegradation organic dye, *Chemosphere.* 274(2021) 129795. <https://doi.org/10.1016/j.chemosphere.2021.129795>.
15. P.T.T. Nguyen, N.H.N. Do, X.Y. Goh, C.J. Goh, R.H. Ong, P.K. Le, N. Phan-Thien, H.M. Duong, Recent Progresses in Eco-Friendly Fabrication and Applications of Sustainable Aerogels from Various Waste Materials, *Waste and Biomass Valorization.* 13 (2022) 1825–1847. <https://doi.org/10.1007/s12649-021-01627-3>.
16. Mohan Seneviratne, Wastewater Treatment Technologies for Textile Industry Wastewater, *Minist. Environ. For. "Guide Assess. Effl. Treat. Plant."* (2016) 119.
17. C. Wang, R. Ma, Z. Huang, X. Liu, T. Wang, K. Chen, Preparation and characterization of carboxymethylcellulose based citric acid cross-linked magnetic aerogel as an efficient dye adsorbent, *Int. J. Biol. Macromol.* 181 (2021) 1030–1038. <https://doi.org/10.1016/j.ijbiomac.2021.04.078>.
18. J. Min, X. Xu, J.J. Koh, J. Gong, X. Chen, J. Azadmanjiri, F. Zhang, S. Liu, C. He, Diverse-shaped tin dioxide nanoparticles within a plastic waste-derived three-dimensional porous carbon framework for super stable lithium-ion storage, *Sci*